0026-895X/92/050922-09$03.00/0

MOLECULAR PHARMACOLOGY, 42:922-930

Nuclear Magnetic Resonance Spectroscopy and Pattern Recognition Analysis of the Biochemical Processes Associated with the Progression of and Recovery from Nephrotoxic Lesions in the Rat Induced by Mercury(II) Chloride and 2-Bromoethanamine

E. HOLMES, F. W. BONNER, B. C. SWEATMAN, J. C. LINDON, C. R. BEDDELL, E. RAHR, and J. K. NICHOLSON

Department of Chemistry, Birkbeck College, University of London, London WC1H 0PP, UK (E.H., J.K.N.), Department of Toxicology, Sterling Winthrop Research UK, Alnwick, Northumberland, NE66 1JH, UK (F.W.B.), and Department of Physical Sciences, The Wellcome Research Laboratories, Beckenham, Kent, BR3 3BS, UK (B.C.S., J.C.L., C.R.B., E.R.)

Received March 25, 1992; Accepted June 3, 1992

SUMMARY

Nephrotoxic lesions were induced in Fischer 344 rats using $HgCl_2$, a proximal tubular toxin, and 2-bromoethanamine (BEA), a medullary toxin. Biochemical effects of these toxins on urinary composition were observed by high resolution ^1H NMR spectroscopy over 9 days after dosing. The onset of, progression of, and recovery from the induced toxic lesions were also followed histopathologically and related to the perturbed urinary biochemistry. Urinary concentrations of 20 endogenous substances were measured simultaneously by NMR at eight time points, to provide a time-related 20-dimensional description of the urinary biochemistry for each rat. Principal components analysis and nonlinear mapping were used to reduce the biochemical parameter spaces for each rat to two or three dimensions for display and classification purposes. An investigation of alternative data-presentation methods was made, and taking interanimal means of the map coordinates at each time point yielded a novel type of metabolic trajectory diagram with which the biochemical abnormalities associated with the $HgCl_2$ and BEA lesions could be related to the progression and recovery phases of the toxic lesions. The time-course trajectories showed characteristically different paths for each toxin. These trajectories allowed the time points at which there were maximum metabolic differences to be determined and provided the visualization of net movements of the treatment group populations in time in relation to interanimal variation. Control animal urine samples subjected to this analysis showed simple clustering, with no evidence of metabolic trajectory. The trajectory for BEA showed different routes for onset of and recovery from toxicity, whereas for $HgCl_2$ the outward trajectory (onset) mapped a space similar to the inward trajectory (recovery phase). This suggests that the NMR-detectable biochemical abnormalities after mercury toxicity mainly reflect the proportions of functional cells lining the nephron, whereas the biochemical abnormalities associated with renal medullary insult probably relate to functional integrity. An examination has been made for those metabolites that are most responsible for defining the trajectories, i.e., the discrimination of renal cortical and medullary toxicity from each other and from controls. These discriminatory metabolites (using paired t test, $p < 0.001$) included valine, taurine, trimethylamine *N*-oxide, and glucose for $HgCl_2$ and acetate, methylamine, dimethylamine, lactate, and creatine for BEA, whereas citrate, succinate, *N*-acetyl resonances from as yet unidentified metabolites, hippurate, alanine, and 2-oxoglutarate played an important role in defining the biochemically perturbed trajectory of both toxins. This approach to the investigation of time-course responses after toxic insult should be widely applicable to other toxin classes, because it allows the analysis of a multitude of biochemical parameters to be related to pathology.

^1H NMR spectroscopy of urine has been shown to yield much information on the concentrations of endogenous metabolites and on their variation in pathological states (1). Therefore, it has been widely applied to toxicity studies on a wide range of toxins, including $CdCl_2$, $HgCl_2$, hexachlorobutadiene, 4-aminophenol, hydrazine, BEA, propyleneimine, and others (2–6). One advantage of using ^1H NMR spectroscopy for body fluid analysis is that it enables a multiparametric data set to be constructed for each time point in a toxicity study in humans

We thank the Science and Engineering Research Council and Sterling Winthroe for the provision of a Cooperative Award in Science and Engineering Studentship (E.H.).

ABBREVIATIONS: BEA, 2-bromoethanamine hydrochloride; PCA, principal components analysis; NLM, nonlinear map; TSP, 3-trimethylsilyl-1-[2,2,3,3-$^2H_4$]propionate; PC, principal component; PR, pattern recognition; MA, methylamine; DMA, dimethylamine; DMG, dimethylglycine; 2-OG, 2-oxoglutarate; TMAO, trimethylamine *N*-oxide; RPN, renal papillary necrosis; NAc, *N*-acetyl.

and animals, with no deliberate bias from preselection of metabolic parameters. Thus, it is possible to simultaneously monitor a wide range of metabolic and biochemical perturbations over a time course after the onset of a toxic insult, which may give considerable insight into the site of action and mechanism of toxicity, even though sensitivity and resolution limitations may, of course, preclude ready observation of some metabolites of interest.

$HgCl_2$ is a nephrotoxin that targets the terminal segment of the proximal tubules (S2 and S3 or straight thick descending limb of the loop of Henle). The primary effects of $HgCl_2$ include necrosis of the convoluted proximal tubule, impairing the reabsorption of low molecular weight proteins, amino acids, glucose, Na^+, K^+, and phosphate (increased in urine) and altering the secretion of hippurate and uric acid (reduced in urine) (2, 7). NMR spectra of urine 24 hr after $HgCl_2$ treatment has previously shown increases in glucose, lactate, and alanine and a decrease in Krebs' cycle intermediates (succinate, 2-OG, and citrate). However, the exact proportions of metabolites may differ considerably according to metabolic states, e.g., during fasting (7). BEA is also a nephrotoxin but targets the renal papilla, giving rise to several clinical features often associated with analgesic nephropathy and resulting in RPN (8, 9). RPN has been partially characterized using ^1H NMR spectroscopy of urine, which showed a depletion of urinary TMAO, DMA, citrate, and 2-OG, with later elevation of succinate and acetate (8). A recovery study has shown there to be different responses in terms of clinical chemistry and histopathology after BEA- and $HgCl_2$-induced nephrotoxicity, and ^1H NMR urinalysis studies on both toxins demonstrated two distinctive patterns of perturbation in metabolic profile after the respective toxic insults (8).

PR is a general term defining a method of data analysis that can classify discrete or scored data as well as quantitative data. PR analysis is performed using a multidimensional parameter space and can be displayed using dimension-reduction techniques. NLM techniques present data values as coordinates in n-dimensional space and compress these typically to a two- or three-dimensional approximation to the multidimensional interpoint distances (10). PCA is an alternative technique of dimension reduction (11), with each PC being a linear combination of the original variables with appropriate weighting coefficients. All PCs are calculated such that they are orthogonal with all other PCs. The first PC contains the largest proportion of variance in the data set, with subsequent PCs containing progressively smaller amounts of variance. Therefore, a plot of the first and second PCs may have negligible contributions from some of the input parameters but may contain a significant proportion of the information content of the original data set. We previously showed that PR methods can be used to classify the toxicities of a variety of compounds based on the analysis of NMR-derived metabolite excretion scores (12–14) and that dose-response effects, sex influences, and nutritional influences on toxin-induced biochemical effects could be studied. We also observed that, by transforming the data from metabolite dimensions to correlation-related dimensions and selecting maximal effects, some of the magnitude variation associated with different doses or different times could be suppressed, enabling characteristic toxin patterns to be better obtained. Because in the present studies it is the time dependencies of metabolite change that are of particular interest, this preprocessing was not used.

Materials and Methods

Animal groups and treatments. Sixty-nine male Fischer 344 rats were housed individually in metabolism cages and allowed free access to food and water throughout the study. The animals were subjected to regular light cycles (7:00 a.m. to 7:00 p.m.). Each animal received a single intraperitoneal dose of either BEA in saline (150 mg/kg, n = 23), $HgCl_2$ in saline (0.75 mg/kg, n = 23), or saline (0.9%, n = 23). Three animals from each of the three groups were killed on days 1, 2, 3, 5, and 9. One animal in the $HgCl_2$-treated group died during the study, leaving 8, 7, and 8 animals in the BEA-treated, $HgCl_2$-treated, and control groups, respectively, that were followed by NMR urinalysis throughout the entire experimental period. Urine was collected over ice at the following time points: predose (16-hr period, T1), 0–8 hr (T2), 8–24 hr (T3), 24–32 hr (T4), 32–48 hr (T5), day 3 (16-hr period, T6), day 5, (16-hr period, T7), and day 9 (16-hr period, T8). On collection, urinary volumes were recorded and urine was centrifuged at 3000 rpm for 10 min in order to remove contaminants. A volume of urine from each sample amounting to twice the urinary flow/hr was lyophilized and reconstituted in deuterium oxide, to which a known amount of TSP (an internal standard, δ = 0 ppm) was added.

^1H NMR spectroscopy. Each urine sample was placed in a 5-mm NMR tube and ^1H NMR spectra were recorded on a Bruker WH400 spectrometer at ambient probe temperature (298 ± 1 K). Typical ^1H NMR parameters were a pulse width of 45°, an acquisition time of 2.0 sec, a spectral width of 5000 Hz, and a delay of 2.5 sec between pulses in order to ensure full T_1 relaxation. The residual water signal was eliminated by the application of a secondary gated irradiation field applied at the resonance frequency of water. Sixty-four free induction decays were collected into 16,384 data points. Before Fourier transformation, the data were zero filled to 32,768 and an exponential apodization function equivalent to 0.5-Hz line-broadening was applied. Resonance assignments of metabolites were confirmed by consideration of chemical shifts, spin-spin coupling patterns, and coupling constants and, ultimately, by standard additions. Three unassigned resonances were also used; these occurred at δ 2.01 and δ 2.07 (arising from the NAc groups of unidentified molecules such as N-acetylated amino acids) and at δ 3.31 (where a singlet was assigned to an unidentified N-trimethyl group, based on the closeness of its ^1H chemical shift to those of other similar molecules).

Although peak heights are not a highly precise measure of concentration because of, for example, line-width effects, in relation to the biological and toxin-induced variation they are an adequate measure. Thus, the peak heights of these 20 defined endogenous metabolite signals were measured (see Table 1) and the concentrations and excretion rates were determined from the relative peak height of the TSP standard, taking into account the number of protons generating the selected signals, the coupling multiplicity, and the urine flow rate with respect to each metabolite. Values were expressed as μmol/kg of body weight/hr and entered into a data table before PR analysis.

Data analysis. Data tables were generated using the software program RS/1 (15) and were analyzed on a DEC VAX8550 computer using the software program ARTHUR (16). PR deals with a multidimensional parameter space, with the excretion rate of each metabolite representing one dimension. The resulting n-dimensional map is displayed in either two- or three-dimensional form by a statistical method of dimension reduction (17). Two types of map were produced; NLM and PCA maps. Before analysis, all data were divided by the corresponding values in the predose period (T1) and were expressed as base-10 logarithms and autoscaled. The metabolites that contributed most to separating the individual time points for a given toxin were determined through the calculation of Fisher or variance weights, with probabilities assessed by paired t tests (16). The selected metabolites

TABLE 1
Metabolite resonances used in the PR analysis

Metabolite	Resonance used	Chemical shift (δ)	Multiplicity
Valine	CH_3	0.96	Doublet
Lactate	CH_3	1.38	Doublet
Alanine	CH_3	1.47	Doublet
Acetate	CH_3	1.95	Singlet
NAc (δ 2.01) (NAc1)	CH_3	2.10	Singlet
NAc (δ 2.07) (NAc2)	CH_3	2.17	Singlet
Succinate	CH_2	2.41	Singlet
2-OG	CH_2	2.44	Triplet
MA	CH_3	2.61	Singlet
Citrate	CH_2	2.50, 2.65	AB
DMA	$(CH_3)_2$	2.72	Singlet
Creatinine	CH_3	3.05	Singlet
Creatine	CH_3	3.01	Singlet
DMG	$(CH_3)_2$	2.93	Singlet
TMAO	$(CH_3)_3$	3.27	Singlet
Taurine	CH_2-NH	3.36	Triplet
Hippurate	CH_2	7.84	Doublet
Glucose	CH	5.20	Doublet
U	$(CH_3)_3$	3.31	Singlet
Betaine	$(CH_3)_3$	3.23	Singlet

were used to generate additional maps to examine whether tighter clusters were formed at each time point. The map-coordinate mean for the various animals at each time point was used to delineate the biochemical trajectory.

Renal histopathology. Animals were killed 1, 2, 3, 5, or 9 days after $HgCl_2$ and BEA treatment. Their kidneys were removed under deep anesthesia, fixed in Formol-saline, dehydrated, embedded in wax, and stained for histological study, using hematoxylin and eosin.

Results

^{1}H NMR analysis of urine. Typical partial 400-MHz ^{1}H NMR spectra of the urine samples from control, $HgCl_2$-treated, and BEA-treated rats are shown in Fig. 1 for the period 8–24 hr after dosing. Clearly there are major changes for a number of metabolites in the two toxin-treated groups, compared with control. The excretion rates have been calculated for 20 defined metabolites for each animal in the control, $HgCl_2$-treated, and BEA-treated groups at eight time points up to 9 days after dosing and including predose values. The mean values for both $HgCl_2$- and BEA-treated rats are given in Table 2. Examination of the spectra and Table 2 shows that for both $HgCl_2$- and BEA-treated rats the metabolic profile becomes increasingly abnormal with time but in general ultimately returns to control-like values by day 5.

For the $HgCl_2$-treated animals, the amino acid valine shows an early increase from the predose level that declines again by day 6. Lactate, alanine, and glucose levels behave similarly, showing an increase at 8–24 hr and a subsequent decline, but with an additional peak at day 3. Elevation of other amino acids such as lysine, isoleucine, and glutamine were also noted in the spectra between 24 hr and 3 days after dosing. In general, these molecules gave rise to low intensity resonances that were difficult to quantify accurately. They have been used in earlier PR analyses involving scored data (13) but were not used in the present PR study because of the difficulty of accurate quantitation. In addition, accurate estimations of some metabolites were made using acidified urine samples at a pH where resonances that are normally overlapped were well separated. Of the organic acids, acetate increases by 8–24 hr after dosing, showing a somewhat variable level but tending to be above control, whereas succinate decreases at 0–8 hr after dosing, recovers subsequently, and drops to below the detection limit before returning to control levels by day 3 and thereafter; 2-OG mirrors the behavior of succinate. Citrate decreases from control levels for up to 48 hr after dosing and then returns to control levels. Taurine decreases to an undetectable level by 48 hr after dosing and then increases beyond the control level on day 3 before declining. Hippurate shows a somewhat similar behavior, by decreasing from control in the period 24–48 hr after dosing before recovering. Both DMA and DMG show a dip to a low level in the period 24–48 hr after dosing. Similarly, the NAc1 and NAc2 resonances also show a dip at the 32–48-hr time period before recovering, whereas the U resonance increases in the 8–24-hr post-dose period before later decreasing.

Examination of the NMR spectra and Table 2 for the BEA-treated animals shows that some metabolites change in common with $HgCl_2$-treated rats but that others also differ. A consistent finding with the BEA-treated rats was the excretion of glutaric (or pentan-1,5-dioic) acid in the 0–8-hr and 8–24-hr periods after dosing. Although glutaric aciduria is a recognized biochemical defect associated with some specific deficiency in dicarboxylic acid-metabolizing enzyme systems (18), it is not known whether this represents a BEA-induced biochemical lesion or whether BEA can be ultimately metabolized to glutaric acid. Given that the glutaric acid could possibly involve a BEA metabolite, it has been excluded as a descriptor from the present PR studies. Lactate and alanine exhibit an early increase, peaking at 8–24 hr after dosing, after which the levels decline. Acetate and the NAc1 resonance also show an increase but both peak on day 3. On the other hand, the NAc2 resonance decreases on day 3 but recovers thereafter. Succinate and 2-OG both exhibit decreases after dosing but show a subsequent increase on day 3 with a later decline. Citrate and hippurate, conversely, show a decreased excretion on day 3 and a subsequent recovery with, incidentally, broadening of the citrate resonances. Creatine is not detectable before dosing but shows a high level in the first 24 hr after dosing, declining again to undetectability. Creatinine also shows an early increase at 24–32 hr after dosing, with a subsequent decline. MA increases after dosing but decreases to control level by day 9. DMA and TMAO behave similarly, showing a decline at 32–48 hr after dosing, with a minimum level on day 3. The U resonance also shows changes that are somewhat variable, in that the level is somewhat elevated at 24–32 hr after dosing, is significantly reduced by day 3, and then shows a later rise but is still below predose levels.

Renal histopathology. $HgCl_2$-treated rats showed extensive degeneration and necrosis of the proximal convoluted tubule (S2 and S3) on days 1 and 2, associated with the formation of hyaline casts in the papilla. Basophilic necrosis was most substantial between days 3 and 5, whereas dramatic tubular regeneration was observed between days 3 and 9, characterized by the appearance of flattened pale-staining cells lining the segments of the damaged tubule. The detailed microscopic pathology of the proximal tubules appeared similar to that reported by others (19, 20).

In BEA treated-animals, tubular necrosis was prominent in the papilla principally in the first 48 hr after dosing. Interstitial necrosis was apparent, although less marked than tubular necrosis, from days 1 to 6 after dosing. Epithelial regeneration

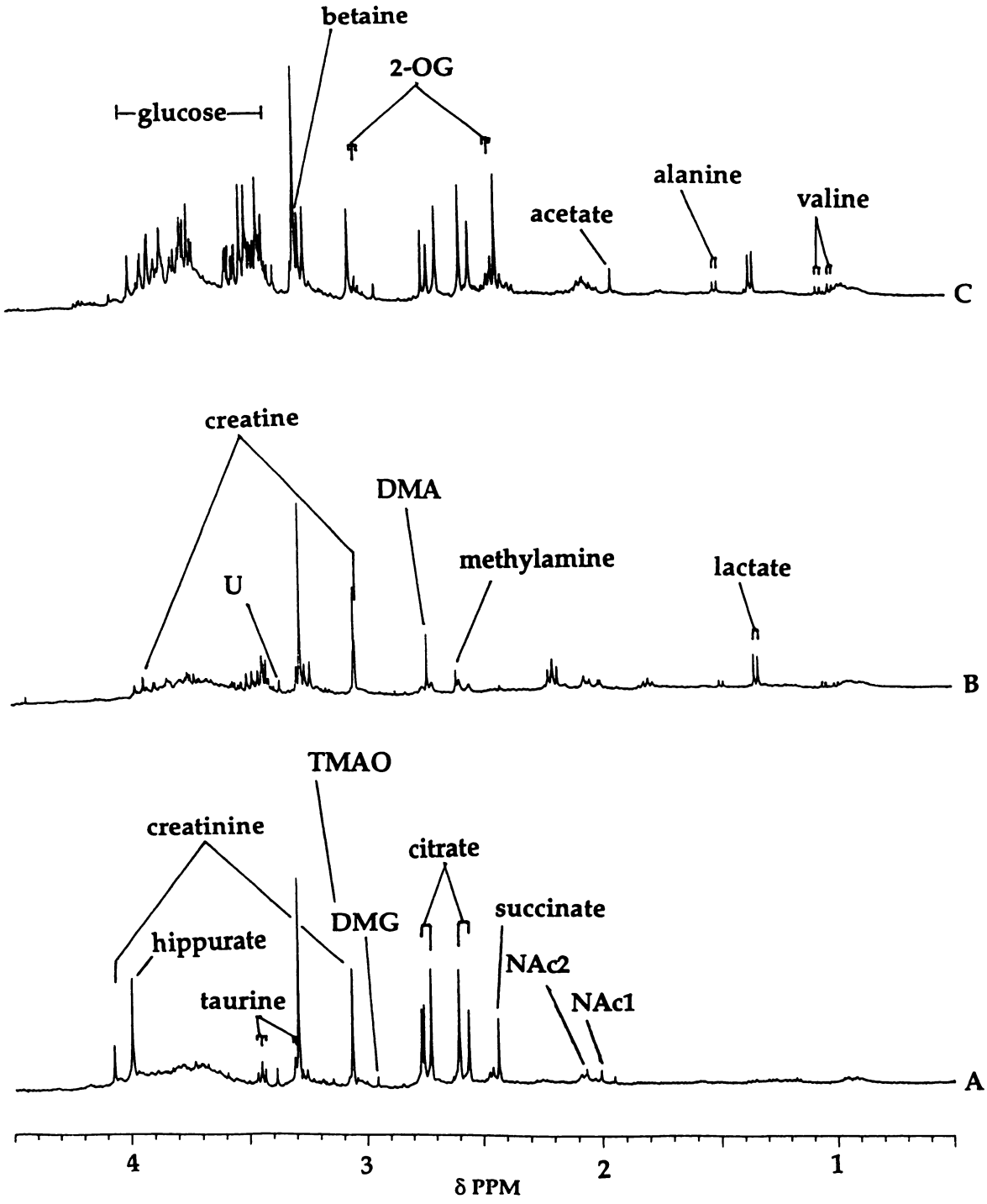

Fig. 1. Partial 400-MHz ^{1}H NMR spectra of rat urine taken 8–24 hr after dosing. A, Control; B, BEA-treated; C, $HgCl_2$-treated.

processes, as evidenced by the formation of new immature cells formed along the tubular basement membranes, were most active in the papilla after BEA treatment between days 2 and 5. Renal cortical necrosis was also apparent from day 3, being most prominent on day 5. Those animals showing most advanced RPN were also found to show the greatest cortical damage. The detailed medullary pathology in the earlier stages of the lesion was similar to that reported by others (21, 22).

Metabolite excretion rate data analysis using PR. The NLM and PCA plots for BEA and $HgCl_2$ (the spread of the control animal data for a given time point was similar) for each animal at each time point, classified by 20 metabolic dimensions, are shown in Fig. 2. Each animal at a given time point is connected to the mean coordinates for that time point, thus producing a "star" effect and giving an indication of scatter. The PCA was found to give a tighter cluster of points around each mean, and both methods demonstrate a similar time-course trajectory for each toxin. The means for controls and both groups at each time point were plotted on a single map in order to show a characteristic trajectory describing the time course of a nephrotoxic episode. The three time course trajectories are combined in Fig. 3 in both NLM and PCA form.

TABLE 2

Mean metabolite excretion rates after treatment of rats with BEA or $HgCl_2$

Values are mean ± standard error.

Metabolite	Excretion rate							
	Pre-dose	0–8 hr	8–24 hr	24–32 hr	32–48 hr	Day 3	Day 5	Day 9
	μmol/kg of body weight/hr							
BEA (150 mg/kg)[a]								
Valine	ND[b]	ND	0.2 ± 0.2	ND	0.7 ± 0.4	0.5 ± 0.4	ND	ND
Lactate	2.5 ± 0.1	5.6 ± 3.1	24.4 ± 2.1	11.7 ± 3.1	5.1 ± 0.4	10.5 ± 4.4	2.4 ± 1.0	0.4 ± 0.2
Alanine	0.2 ± 0.2	2.0 ± 1.4	4.1 ± 1.0	1.2 ± 0.8	1.2 ± 0.3	2.2 ± 1.4	3.6 ± 0.5	ND
Acetate	2.2 ± 0.5	29.6 ± 17.0	0.6 ± 0.2	6.2 ± 3.6	1.0 ± 1.2	36.9 ± 6.5	1.0 ± 0.3	0.4 ± 0.2
NAc1	3.1 ± 0.4	7.8 ± 3.3	2.6 ± 0.8	5.6 ± 1.5	2.0 ± 0.2	6.7 ± 0.4	2.8 ± 0.8	1.4 ± 0.3
NAc2	2.6 ± 0.6	12.3 ± 5.3	2.9 ± 0.8	5.8 ± 1.6	2.0 ± 0.2	0.5 ± 0.1	3.6 ± 0.8	1.5 ± 0.4
Succinate	18.7 ± 1.9	7.6 ± 3.0	1.2 ± 0.4	2.5 ± 0.8	4.6 ± 0.8	28.8 ± 0.6	15.3 ± 3.4	5.8 ± 0.6
2-OG	19.4 ± 4.2	3.4 ± 1.3	ND	2.0 ± 1.2	1.7 ± 1.1	4.2 ± 1.0	28.2 ± 7.1	11.2 ± 10.6
Citrate	135.2 ± 16.8	96.5 ± 27.8	64.4 ± 50.8	25.2 ± 5.2	22.7 ± 5.2	4.1 ± 2.2	110.7 ± 16.0	61.0 ± 12.4
MA	0.9 ± 0.1	3.2 ± 1.2	5.4 ± 1.4	5.5 ± 1.3	2.9 ± 0.5	0.5 ± 0.2	1.0 ± 0.2	0.3 ± 0.1
DMA	7.8 ± 1.3	13.7 ± 4.6	7.1 ± 1.4	7.0 ± 1.0	4.1 ± 0.5	1.2 ± 0.4	8.5 ± 2.0	3.0 ± 1.3
DMG	2.5 ± 0.3	1.7 ± 0.8	0.2 ± 0.1	5.5 ± 4.7	0.4 ± 0.0	0.4 ± 0.2	1.0 ± 0.2	0.4 ± 0.1
Creatine	ND	23.9 ± 13.0	25.2 ± 6.8	13.4 ± 10.6	22.0 ± 3.2	5.8 ± 1.7	ND	ND
Creatinine	27.5 ± 2.9	41.4 ± 16.4	36.1 ± 8.7	92.2 ± 18.2	23.9 ± 2.8	12.4 ± 2.2	19.4 ± 3.8	11.1 ± 0.3
Betaine	1.2 ± 0.7	24.6 ± 22.1	10.5 ± 3.6	ND	2.8 ± 1.4	ND	0.2 ± 0.2	ND
TMAO	22.0 ± 2.8	11.8 ± 4.8	13.1 ± 3.2	17.5 ± 4.6	7.9 ± 1.1	1.0 ± 0.6	13.2 ± 2.8	6.7 ± 1.2
U	3.2 ± 0.8	1.5 ± 0.3	3.1 ± 0.8	6.0 ± 0.2	1.3 ± 0.2	0.1 ± 0.1	1.6 ± 0.4	0.7 ± 0.2
Taurine	34.5 ± 4.8	71.0 ± 45.4	21.1 ± 13.0	62.5 ± 22.7	30.6 ± 6.4	1.9 ± 0.6	21.6 ± 6.6	5.4 ± 2.1
Glucose	3.8 ± 1.5	7.0 ± 0.3	4.3 ± 2.7	1.0 ± 0.2	1.0 ± 0.7	0.2 ± 0.2	2.3 ± 1.2	2.4 ± 0.2
Hippurate	60.7 ± 25.8	12.1 ± 2.4	15.9 ± 3.9	20.2 ± 4.4	20.1 ± 2.8	2.8 ± 0.3	34.4 ± 9.6	12.1 ± 2.6
$HgCl_2$ (0.75 mg/kg)[c]								
Valine	0.2 ± 0.1	ND	16.4 ± 5.9	10.1 ± 1.7	10.2 ± 2.5	13.2 ± 3.1	0.3 ± 0.2	0.1 ± 0.0
Lactate	1.5 ± 1.1	7.0 ± 4.4	124.0 ± 33.5	43.5 ± 9.8	43.5 ± 8.8	167.8 ± 42.0	25.0 ± 16.0	5.9 ± 3.4
Alanine	0.7 ± 0.6	0.4 ± 0.4	22.4 ± 7.4	18.2 ± 4.6	22.8 ± 7.0	67.5 ± 10.6	2.3 ± 0.6	0.8 ± 0.6
Acetate	3.0 ± 0.6	1.0 ± 0.3	11.4 ± 2.3	2.8 ± 1.2	9.8 ± 3.1	7.7 ± 1.4	1.9 ± 0.4	4.0 ± 2.2
NAc1	2.4 ± 0.5	3.4 ± 1.2	3.8 ± 1.4	1.8 ± 0.7	ND	5.6 ± 1.2	1.8 ± 0.3	2.0 ± 0.6
NAc2	3.6 ± 0.4	2.3 ± 1.0	2.4 ± 1.1	1.1 ± 1.4	ND	7.1 ± 1.4	1.4 ± 0.3	2.8 ± 1.2
Succinate	20.9 ± 4.5	5.8 ± 0.8	26.8 ± 3.5	ND	0.3 ± 0.2	16.7 ± 4.0	17.3 ± 3.1	13.9 ± 5.2
2-OG	15.7 ± 3.7	9.7 ± 1.8	37.2 ± 10.4	ND	ND	72.2 ± 13.8	21.0 ± 3.7	25.6 ± 7.6
Citrate	123.1 ± 26.9	71.5 ± 5.9	155.9 ± 77.0	28.6 ± 5.4	24.1 ± 6.3	259.1 ± 59.4	113.1 ± 19.3	143.5 ± 10.7
MA	9.7 ± 7.8	0.8 ± 0.4	0.5 ± 0.1	ND	0.0 ± 0.0	0.8 ± 0.6	0.5 ± 0.2	0.7 ± 0.6
DMA	13.4 ± 2.5	29.4 ± 7.2	10.5 ± 2.1	2.1 ± 0.6	1.0 ± 0.4	19.6 ± 1.7	7.1 ± 1.6	4.7 ± 5.3
DMG	3.3 ± 0.5	1.2 ± 0.6	3.0 ± 0.6	0.9 ± 0.4	1.3 ± 0.4	6.2 ± 1.2	2.9 ± 0.6	2.0 ± 0.7
Creatine	ND	ND	ND	ND	ND	ND	ND	ND
Creatinine	31.3 ± 5.2	29.4 ± 7.3	39.6 ± 10.6	14.0 ± 3.7	13.8 ± 4.4	59.7 ± 14.2	20.2 ± 4.0	18.0 ± 5.3
Betaine	ND	17.1 ± 7.2	13.8 ± 7.7	ND	ND	3.2 ± 2.0	1.0 ± 0.6	1.2 ± 0.9
TMAO	24.7 ± 6.3	11.7 ± 0.8	30.6 ± 7.4	16.2 ± 2.5	8.5 ± 3.1	35.0 ± 6.3	15.8 ± 3.2	12.2 ± 3.4
U	1.8 ± 0.3	1.4 ± 0.3	11.9 ± 2.5	7.4 ± 1.8	5.7 ± 1.5	10.5 ± 3.7	1.2 ± 0.3	0.4 ± 0.3
Taurine	33.9 ± 7.0	41.5 ± 9.2	ND	ND	ND	102.4 ± 24.2	8.4 ± 5.2	8.8 ± 2.6
Glucose	2.8 ± 1.2	0.6 ± 0.6	93.2 ± 31.4	23.6 ± 5.0	20.1 ± 4.6	115.7 ± 37.1	3.4 ± 1.6	17.5 ± 4.5
Hippurate	41.0 ± 10.6	20.2 ± 5.0	39.3 ± 11.2	5.5 ± 1.3	5.7 ± 2.4	37.7 ± 9.8	27.7 ± 8.3	8.8 ± 2.6

[a] $n = 8$.
[b] ND, not detected.
[c] $n = 7$.

These constructed metabolic trajectories clearly follow the course of the pathological lesions, with a period showing severe disturbances in metabolic profile corresponding to the maximal time of damage (2–3 days after dosing), a period of less severe perturbation corresponding to the regenerative phases of the lesion (4–5 days after dosing), and a rapid return towards the control biochemical profile as the regenerated epithelial cells become more functionally efficient (days 7 and 8). BEA and $HgCl_2$ showed significantly different trajectories, particularly in the PCA map. The trajectory for $HgCl_2$ progressed away from the control cluster of means and then returned, retracing a path similar to that produced during the development of the lesion. However, the BEA trajectory moved from control points but returned via a different path, defining a figure of eight pattern. A three-dimensional version of the PCA plot is given in Fig. 4. Whereas the control means are clustered together, the $HgCl_2$ and the BEA trajectories extend in very different directions, indicating that PC3 is also a valuable discriminator in defining the trajectories. This is also supported by the observation that the contribution to the variance from the individual PCs is PC1 = 26.5%, PC2 = 17.1%, and PC3 = 11.7%.

Region-specific nephrotoxicity results in the expression of characteristic urinary markers of toxicity that have been studied previously using NMR (2). Fisher or variance weights for control and toxin-treated groups were calculated between different time points. It was observed that in many instances a Fisher weight in excess of 5 was observed and a paired t test further supported the proposal ($p < 0.001$) that certain metabolite values were significantly different between certain time points, according to the control or toxin experiment under study. Whereas Fisher or variance weights involve intergroup comparisons, the paired t test retains intra-animal differences. Because all data had been divided by corresponding T1 values, the statistical analysis here excludes comparisons with T1.

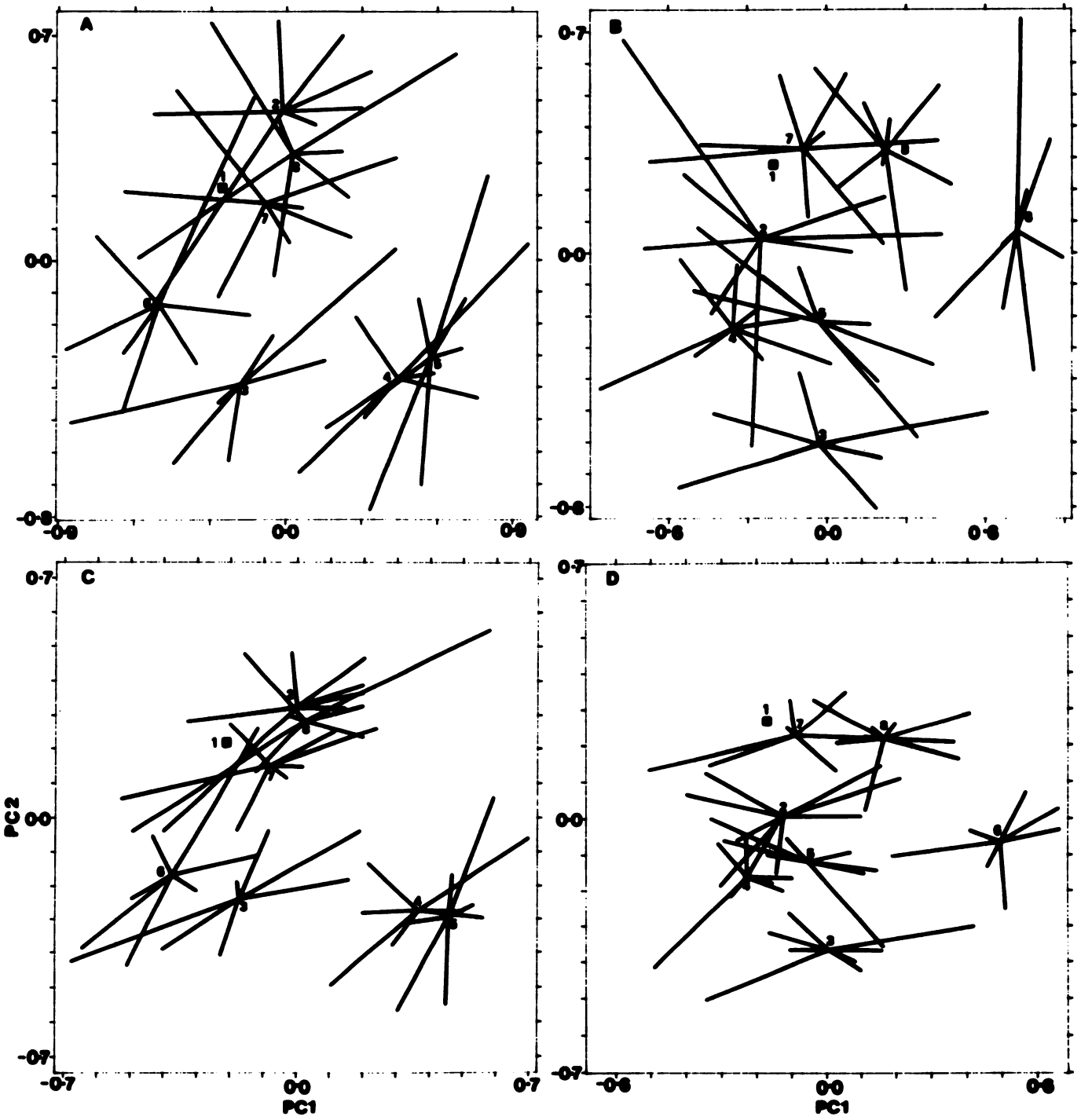

Fig. 2. NLMs for $HgCl_2$-treated (A) and BEA-treated (B) rats and corresponding PCA maps for $HgCl_2$-treated (C) and BEA-treated rats (D). Each time point comprises seven animals for $HgCl_2$ and eight animals for BEA. The means for each time point have been plotted and each individual animal result has been joined to the mean. All values are relative to those at T1; therefore, all animals map to a single point at T1 (□). Each data set was autoscaled separately.

Table 3 represents, for time points T2 to T8, those metabolites that change between time points ($p < 0.001$) and the direction of change with time. For control, BEA-treated, and $HgCl_2$-treated groups, 9, 13, and 12 metabolites, respectively, are selected, with some in common between groups (see Table 4). Overall, 19 of the 20 metabolites are selected, indicating that with the exception of DMG all are significantly perturbed. NLM or PC trajectory maps for each of the three groups based on the selected metabolites for each are similar in time-point spread and trajectory to those derived from all 20 metabolites, confirming that the trajectory information is primarily represented in the metabolite subset data. Furthermore, for each group the NLM and PC1 versus PC2 maps are very similar, because proportionally more of the variance was contained in the first two PCs for the restricted metabolite data sets, relative to the full metabolite data sets.

Inspection of Table 3 enables reversal of metabolite perturbations to be readily seen in toxin-treated groups. In contrast,

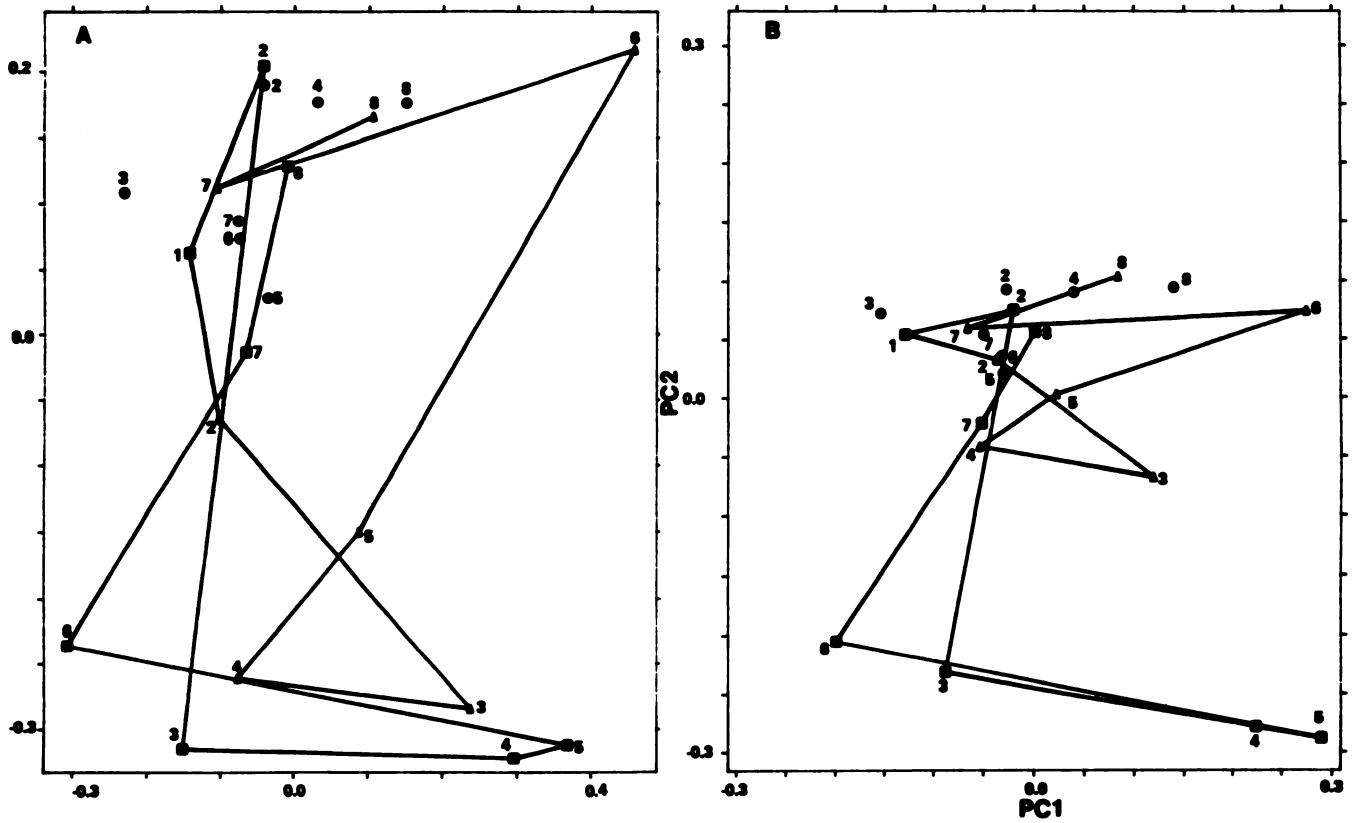

Fig. 3. Combined mean trajectory maps for both toxins and control. A, NLM; B, PCA map. ●, Control group; ■, $HgCl_2$-treated group; ▲, BEA-treated group. Control point means are not linked for clarity.

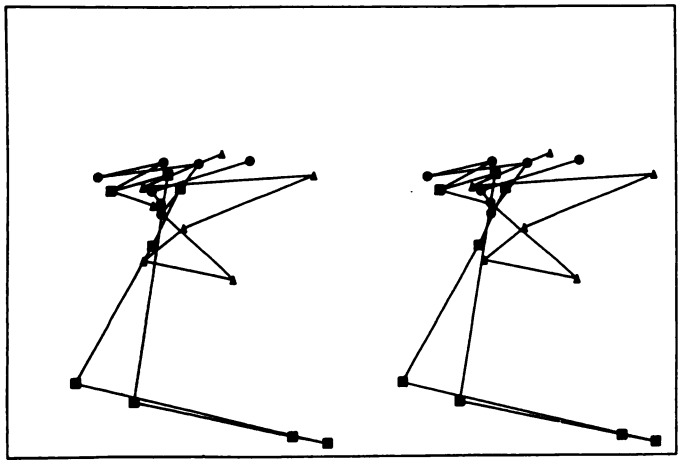

Fig. 4. Three-dimensional PC trajectory maps for both toxins and control, showing linked means. ●, Control group; ■, $HgCl_2$-treated group; ▲, BEA-treated group.

only lactate shows reversal in the control group, but the reason for the decline in the level of several metabolites (e.g., betaine, TMAO, MA, and DMA) beyond 24 hr after dosing is unclear.

Trajectories using an even more restricted metabolite set ($p < 0.0001$), although apparent, were less clear, confirming that variance of individual metabolite levels between animals is high enough to partially obscure the trajectories, whereas a multivariate approach exploits advantageously the information in all of the metabolite data.

Discussion

Biochemical significance of urinary metabolite changes. Progressive changes in the ^1H NMR spectral profiles of urine appear to parallel closely the development of pathological changes caused by exposure to $HgCl_2$ and BEA. This is confirmed by examination of the quantitative excretion data on a large number of metabolites determined by NMR spectroscopy (Table 2). Statistical analysis of these data reveals that each time point after toxin exposure has a characteristically perturbed range of metabolites (Tables 3 and 4).

The earliest change detected after exposure to $HgCl_2$ included a transient reduction in the excretion of the citric acid cycle intermediates succinate, 2-OG, and citrate at 0–8 hr. The excretion of these metabolites then reached a second minimum between 24–32 hr and 32–48 hr after dosing, followed by a dramatic recovery in excretion rate on day 3 (Table 2).

The complex fluctuations in the excretion of these key intermediates probably reflect the changing functionality of tubular mitochondria with time, because inhibition of mitochondrial enzymes, especially succinate and malate dehydrogenases, is a well known effect of $HgCl_2$ (7). The earliest urinary marker of $HgCl_2$-induced nephrotoxicity that is strongly significant is glycosuria, which is very pronounced 8–24 hr after dosing (Tables 2 and 3). However, glycosuria has been shown to be a much weaker marker of $HgCl_2$-induced damaged in treated animals that have been fasted (due to a lower plasma glucose, which raises the apparent overflow threshold for urinary glucose) (7). Interestingly, urinary taurine is significantly depleted 8–48 hr after $HgCl_2$ treatment. The biochemical significance of this is as yet unknown, although it could reflect an increased demand for extra-renal taurine because this amino acid is a precursor in glutathione synthesis. It has been noted previously that taurinuria (i.e., elevated taurine) after toxic insult is a marker of acute liver damage in the rat (5, 23). Amino acids such as valine and alanine are also excreted in much larger

TABLE 3

List of metabolites that differ significantly (paired *t* test, $p < 0.001$) between time points T2 to T8

The arrows indicate the direction of change for increasing time points.

	Control[a]	$HgCl_2$-treated	BEA-treated
T2-T3	NAc1 ↑, Succ ↑	Glc ↑	
T2-T4		Val ↑, 2-OG ↓, Succ ↓	
T2-T5	Lac ↑	Val ↑, 2-OG ↓, Succ ↓, Ala ↑, Glc ↑, NAc1 ↓	
T2-T6	Bet ↓	Ala ↑, Glc ↑	DMA ↓, U ↓, NAc2↓
T2-T7	Lac ↑		
T2-T8	Bet ↓		Ace ↓
T3-T4	MA ↓, TMAO ↓	2-OG ↓, Succ ↓	
T3-T5		2-OG ↓, Succ ↓, Hipp ↓	Lac ↓, 2-OG ↑
T3-T6	Bet ↓	Tau ↑	Ace ↑, 2-OG ↑, Succ ↑, Hipp ↓
T3-T7			Cr ↓, 2-OG ↑
T3-T8	DMA ↓, Cn ↓, TMAO ↓, Hipp ↓	Tau ↑, U ↓	Lac ↓, 2-OG ↑, Ala ↓, MA ↓, Cr ↓
T4-T5			
T4-T6		2-OG ↑, Succ ↑, Cit ↑, Tau ↑	DMA ↓, Cn ↓, Hipp ↓, U ↓
T4-T7		2-OG ↑, Succ ↑, Val ↓, U ↓	
T4-T8		2-OG ↑, Succ ↑, Val ↓, Ala ↓, Tau ↑	Lac ↓, 2-OG ↑, Ala ↓, MA ↓, Cn ↓, U ↓
T4-T6		2-OG ↑, Succ ↑, Cit ↑, Tau ↑, NAc1 ↑, NAc2 ↑	DMA ↓, Ace ↑, Hipp ↓, U ↓
T5-T7		2-OG ↑, Succ ↑, Val ↓, NAc1 ↑, NAc2 ↑	Cr ↓
T5-T8	Lac ↓	2-OG ↑, Succ ↑, Val ↓, Tau ↑, NAc2 ↑, NAc1 ↑	Lac ↓, MA ↓, Cr ↓
T6-T7			Ace ↓, DMA ↑, Hipp ↑, NAc2 ↑
T6-T8		Ala ↓, TMAO ↓, Glc ↓, Tau ↓	Ace ↓, Succ ↓, Cit ↑, U ↑
T7-T8			

[a] Succ, succinate; Glc, glucose; Val, valine; Ala, alanine; Lac, lactate; Bet, betaine; Cn, creatinine; Hipp, hippurate; Tau, taurine; Cit, citrate; Cr, creatine; Ace, acetate.

TABLE 4

List of metabolites for each of the three groups represented in Table 3 (paired *t* test, $p < 0.001$, T2-T8)

Control	BEA-treated	$HgCl_2$-treated
MA	MA	
DMA	DMA	
TMAO		TMAO
Betaine		
NAc1		NAc1
Creatinine	Creatinine	
Hippurate	Hippurate	Hippurate
Succinate	Succinate	Succinate
Lactate	Lactate	
	Citrate	Citrate
	2-OG	2-OG
	Acetate	
	U	U
	Creatine	
	NAc2	NAc2
	Alanine	Alanine
		Glucose
		Valine
		Taurine

quantities from 8 hr to 3 days after $HgCl_2$ dosing, corresponding to failure of the proximal tubule to reabsorb these from the primary urinary ultrafiltrate. These have previously been identified as strong urinary markers (7). Profound lactic aciduria appears to be a general marker for severe renal cortical necrosis, which is associated with reduced cortical blood flow and a reduction in Krebs' cycle activity (7, 24).

The biochemical changes associated with BEA-induced RPN are of considerable interest because there are no established clinical markers for RPN caused by use of nonsteroidal anti-inflammatory drugs in humans. In an earlier NMR study we reported semiquantitative measurements on changes in the excretion profiles of DMA, TMAO, succinate, and acetate after BEA insult (2). The data presented in Tables 2 and 3 suggest that there is indeed a characteristic combination of low molecular weight excretion markers of RPN to be found in the urine. This is further exemplified in the PR analysis of the data (see below). In particular, early markers of BEA-induced medullary damage include an increase in the excretion of DMA, acetate, betaine, creatine, and two as yet unidentified but probably *N*-acetylated metabolites (NAc1 and NAc2). It is possible that these putative NAc signals are related to an increased rate of excretion of glycosaminoglycans, which are present at high concentrations in the renal medullary interstitium and may be lost to the urine when cell damage occurs. We have previously shown that the NAc groups of sialic acid residues of plasma glycoproteins (such as α_1 acid glycoprotein) give sharp signals at δ ~2.0–2.1 because the side chains are largely motionally unconstrained, with consequent long proton T_2 relaxation times (25). Complex fluctuations in the levels of these and several other metabolites (e.g., Krebs' cycle intermediates and hippurate) then follow as the lesion progresses and recovers (Tables 2 and 3). These are difficult to interpret directly because there is also slight secondary cortical damage after BEA treatment. The early elevation of DMA and betaine (in the absence of glycosuria and amino aciduria) is probably characteristic of RPN. The renal medulla contains very high levels of these compounds, which function as osmoprotective agents (osmolytes) and help to ameliorate the denaturing effects of high osmolarity on medullary enzymes (26). Damage to the structural integrity of the renal medulla would be expected to release these compounds (and possibly other as yet unidentified osmolytes) into the urine.

PR analysis of NMR data. PR has provided a novel means of representing the data obtained from ^1H NMR urinalysis after the induction of renal lesions using model nephrotoxins. The NLMs and PCA maps show time-related trajectories that may be related to pathological events. Histopathology showed that in BEA-treated rats papillary necrosis was most severe in

the first 48 hr (T2–T5). The reversible nature of the map trajectory seen for $HgCl_2$ can be explained simply as the functionality of a single type of cell being perturbed as cells die. As new cells are regenerated the functionality returns to normal and the time points on the trajectory map return towards the predose position. This is consistent with the histopathology results, which showed degeneration of the S2 and S3 regions of the proximal tubule followed by regeneration between days 3 and 9. Further evidence to support this single mode of toxicity can be deduced from an analysis of those metabolite descriptors that are significant in discriminating the various time points on the map. Thus, through the various changes in direction, the same metabolites are in general significant, mainly succinate, 2-OG, and valine.

On the other hand, the BEA-induced time-course map trajectory shows different routes for the onset and recovery phases of the study. This could be explained in two ways. Either the cellular functionality due to a single type of toxicity recovers in a nonreversible sense (for example, for the case of two metabolites, A and B, A is lost first followed by B but A recovers first followed by B) or BEA induces at least two types of renal toxicity. Evidence for the latter explanation can be seen in the histopathology; after the initial papillary tubular necrosis seen in the first 48 hr after dosing, cortical necrosis was observed after day 3 of the study. In addition, an examination of the metabolites that are significant in defining the time points on the maps shows that, unlike with $HgCl_2$, different metabolites are significant at different times. The trajectories derived from the NMR urinalysis appear to indicate the developing pathological state before its detection by pathological methods. Both the NLMs and PCA maps produced similar results, although PCA analysis proved to be the more useful method of data analysis in terms of reducing the interanimal variation and defining a clearer trajectory.

Conclusions. These results clearly show that the two toxins investigated each possess a characteristic trajectory, as defined by 20 endogenous parameters, and that these combined parameters define an onset of, progression of, and recovery from a nephrotoxic lesion that is distinctive for that toxin. Whereas the trajectory defining $HgCl_2$-induced toxicity follows a similar path in both the onset and the recovery directions, the BEA trajectory defines a "figure of eight", which may be influenced by the fact that BEA induces mild secondary cortical toxicity as well as RPN.

The possibility now exists of overlaying observed biochemical trajectories in, for example, two or three dimensions on those of known standard toxins, to aid prediction of toxin type by examination of geometric congruence of the toxicological trajectories. This approach of combining ^1H NMR analysis of body fluids taken in time-course studies with PR may be useful in clinical situations in the assessment of a patient's recovery from a toxic episode or a metabolic disease state.

Acknowledgments

We thank The University of London Intercollegiate Spectroscopic Services, The Medical Research Council, and the Science and Engineering Research Council for the provision of centralized high-field NMR facilities.

References

1. Nicholson, J. K., and I. D. Wilson. High resolution proton NMR spectroscopy of biofluids. *Prog. NMR Spectrosc.* **21**:444–501 (1989).
2. Gartland, K. P. R., F. W. Bonner, and J. K. Nicholson. Investigations into the biochemical effects of region-specific nephrotoxins. *Mol. Pharmacol.* **35**:242–250 (1989).
3. Nicholson, J. K., D. P. Higham, J. A. Timbrell, and P. J. Sadler. Quantitative high resolution NMR urinalysis studies on the biochemical effects of cadmium in the rat. *Mol. Pharmacol.* **36**:398–404 (1989).
4. Foxall, P., M. Bending, K. P. R. Gartland, and J. K. Nicholson. Acute renal failure following accidental cutaneous absorption of phenol: application of proton NMR urinalysis to monitor the disease process. *Hum. Toxicol.* **9**:491–496 (1989).
5. Sanins, S. M., J. A. Timbrell, C. Elcombe, and J. K. Nicholson. Proton NMR studies on the metabolism and biochemical effects of hydrazine *in vivo*. *Methodol. Surv. Biochem. Anal.* **18**:375–381 (1988).
6. Bales, J. R., J. D. Bell, J. K. Nicholson, P. J. Sadler, J. A. Timbrell, R. D. Hughes, P. N. Bennet, and R. Williams. Metabolic profiling of body fluids by proton NMR: self-poisoning episodes with paracetamol (acetaminophen). *Magn. Res. Med.* **6**:301–306 (1988).
7. Nicholson, J. K., J. A. Timbrell, and P. J. Sadler. Proton NMR spectra of urine as indicators of renal damage: mercury-induced nephrotoxicity in rats. *Mol. Pharmacol.* **27**:644–651 (1985).
8. Holmes, E., F. W. Bonner, K. P. R. Gartland, and J. K. Nicholson. Proton NMR monitoring of the onset and recovery of experimental renal damage. *J. Pharmaceut. Biomed. Anal.* **8**:959–962 (1990).
9. Sabatini, S. Analgesic induced papillary necrosis. *Semin. Nephrol.* **8**:41–52 (1988).
10. Kowalski, B. R., and C. F. Bender. Pattern recognition: a powerful approach to interpreting chemical data. *J. Am. Chem. Soc.* **94**:5632–5639 (1972).
11. Seal, H. *Multivariate Statistical Analysis for Biologists*. Methuen & Co. Ltd., London, 101–102 (1968).
12. Gartland, K. P. R., S. M. Sanins, J. K. Nicholson, B. C. Sweatman, C. R. Beddell, and J. C. Lindon. Pattern recognition analysis of high resolution ^1H NMR spectra of urine: a non-linear mapping approach to the classification of toxicological data. *NMR Biomed.* **3**:166–172 (1990).
13. Gartland, K. P. R., C. R. Beddell, J. C. Lindon, and J. K. Nicholson. Application of pattern recognition methods to the analysis and classification of toxicological data derived from proton nuclear magnetic resonance spectroscopy of urine. *Mol. Pharmacol.* **39**:629–642 (1991).
14. Gartland, K. P. R., C. R. Beddell, J. C. Lindon, and J. K. Nicholson. A pattern recognition approach to the comparison of PMR and clinical chemistry data for classification of nephrotoxicity. *J. Pharmaceut. Biomed. Anal.* **8**:963–968 (1990).
15. RS/1. BBN Software Products, UK Ltd., Staines, Middlesex, UK (1988).
16. ARTHUR 81, version 4.1. B&B Associates, Seattle, WA.
17. Chatfield, C., and A. J. Collins. *Introduction to Multivariate Analysis*. Chapman and Hall, London, 57–59 (1980).
18. Stanburg, J. B., J. B. Wyngaarden, D. S. Fredrickson, J. L. Goldstein, and M. S. Braun. *The Metabolic Basis of Inherited Disease*. McGraw-Hill, New York, 461–464 (1983).
19. Haagsma, B. H., and A. W. Pound. Mercuric chloride induced renal tubular necrosis in the rat. *Br. J. Exp. Pathol.* **60**:341–352 (1979).
20. Haagsma, B. H., and A. W. Pound. Mercuric chloride induced tubular necrosis in the rate kidney: the recovery phase. *Br. J. Exp. Pathol.* **61**:229–241 (1979).
21. Murray, G., R. G. Wyllie, G. S. Hill, P. W. Ramsden, and R. H. Hepinstall. Experimental papillary necrosis of the kidney. I. Morphologic and functional data. *Am. J. Pathol.* **67**:285–302 (1979).
22. Hill, G. S., R. G. Wyllie, M. Miller, and R. H. Hepinstall. Experimental papillary necrosis of the kidney. II. Electron microscopic and histochemical study. *Am. J. Pathol.* **68**:213–234 (1972).
23. Sanino, S. M., J. A. Timbrell, C. Elcombe, and J. K. Nicholson. Proton NMR studies on the metabolism and biochemical effects of hydrazine *in vivo*. *Methodol. Surv. Biochem. Anal.* **18**:375–381 (1988).
24. Barnes, J. L., E. M. McDowell, J. S. McNeil, W. Flamenbaum, and B. F. Trump. Studies on the pathophysiology of acute renal failure. V. Effect of chronic saline loading on the progression of proximal tubular injury and functional impairment following administration of mercuric chloride. *Virchows Arch. B Cell Pathol.* **32**:233–260 (1980).
25. Bell, J. D., J. C. C. Brown, J. K. Nicholson, and P. J. Sadler. Assignment of resonances for "acute phase" glycoproteins in high resolution proton NMR spectra of human blood plasma. *FEBS Lett.* **215**:311–315 (1987).
26. Bagnasco, S., R. Balaban, H. M. Fales, Y.-M. Yang, and M. B. Burg. Predominant osmotically active organic solutes in rat and rabbit renal medullas. *J. Biol. Chem.* **261**:5872–5877 (1986).

Send reprint requests to: Dr. J. K. Nicholson, Department of Chemistry, Birkbeck College, University of London, Gordon House, 29 Gordon Square, London WC1H 0PP, UK.